https://doi.org/10.31871/IJNTR.8.5.26 International Journal of New Technology and Research (IJNTR)
ISSN: 2454-4116, Volume-8, Issue-5, May 2022 Pages 17-19

Using a Bidirectional Reflectance Model to Normalize Multitemporal Satellite Images

Chien-Hui Liu

***Abstract*—Natural targets reflectance exhibits anisotropic properties of surface, which are angular dependent, including solar and viewing geometries. After atmospheric correction of remotely sensed images, multi-temporal bidirectional reflectance factor shows bidirectional effect and should be normalized to a standardized solar-viewing-target geometry. In this study, a normalization method for multitemporal satellite images is implemented and evaluated. The normalization efficiency is evaluated.**

***Index Terms*—Bidirectional Reflectance Factor, Bidirectional Reflectance Distribution Function, Atmospheric Correction, Remote Sensing.**

I. Introduction

One of the most important global changes is the urbanization. Remote sensing plays a crucial role on the assessment of spatial and temporal patterns of urban growth as well as its impact on the environment [1]. Urban reflectance is one of the key parameter in controlling urban heat island (UHI) effect. White roofs, green roofs and photovoltaic panels are important in reducing UHI effect [2]. Remote sensing of urban reflectance is important in climate change issue.

Due to the anisotropic properties of natural targets, surface reflectances are angular dependent, including solar and viewing geometries. Therefore, bidirectional reflectance factor (BRF) after atmospheric correction (AC) of remotely sensed image should be 'normalized' to a standardized solar-viewing-target geometry (SVTG) such as nadir view and mean solar zenith angle used in Nadir BRDF-Adjusted Reflectances (NBAR) for MODerate Resolution Imaging Spectroradiometer (MODIS) [3]. A specific solar zenith angle for multi-temporal data is also used in standardizing SVTG, such as spring equinox angle at the given test area [4]. These standardized SVTG image is derived based on atmospherically corrected surface reflectances and then bidirectional reflectance distribution function (BRDF) modeling of these reflectances within a short temporal period, such as 16 days defined by MODIS BRDF/Albedo and NBAR products. For high resolution data and limited budget, cloudless and temporal-discontinuous images ranging over years are usually acquired for multi-temporal analysis. Hence, there may be very often less than enough temporal-continuous images, e.g. seven images in full BRDF modeling for MODIS NBAR.

In this study, we implement a normalization method for multi-temporal SPOT data. Normalization procedures contains three steps: (1) atmospheric correction, (2) bidirectional reflectance modeling and (3) normalization of bidirectional reflectance factor [4]. This method derives normalized reflectance by Roujean BRDF [5]. The performance of normalization method is assessed.

Chien-Hui Liu, Department of Digital Media and Product Design, Transworld University, Douliu, Taiwan, R.O.C.

II. Methodology

A. Satellite Images

Tainan test site is selected. Total of 31 SPOT satellite images ranges from 2002/04 to 2011/04. Images with only cloudless and uniform atmospheric effect determined by visual interpretation are acquired. Test area covers 12 km x 12 km wide.

Sunphotometer data are available at Cheng-Kung_Univ station which is part of NASA Aerosol Robotic Network (AERONET) [6]. AOD can be downloaded from AERONET and used in validation of retrieved AOD, which is the key parameter in AC of SPOT images.

B. Atmospheric Correction

Before atmospheric correction of SPOT images, AOD must be known by ground measurement or derivation from image. In this study, AOD is derived from image itself and validated by AERONET. Radiative transfer model 6SV [7], i.e. vector-based 6S, is implemented in AOD retrieval and the follow-on AC. Atmospheric profile of tropic atmosphere is selected. Desert aerosol model and assumed DT reflectance of 0.03 at red band area are used. Lookup table between top-of-atmosphere reflectance and surface reflectance is pre-computed by 6SV. Then it can be used to convert raw image to surface reflectance image, i.e. AC of SPOT image. Surface reflectance is called bidirectional reflectance factor (BRF) due to its angle dependence. Since an error of 0.01 in assumed surface reflectance can cause error of 0.1 in retrieved AOD, accuracy of AC can be estimated as 0.011 [8], [9].

C. Bidirectional Reflectance Modeling

Linear kernel-driven models with three parameters: Roujean BRDF [5], are used to parameterize the bidirectional reflectance for different viewing and solar zenith angles.

Roujean BRDF can be written as follows:

$$\rho(\theta_s,\theta_v,\phi)=k_0+k_1f_1(\theta_s,\theta_v,\phi)+k_2f_2(\theta_s,\theta_v,\phi) \tag{1}$$

$$f_1(\theta_s,\theta_v,\phi)=[(\pi-\phi)\cos\phi+\sin\phi]\tan\theta_s\tan\theta_v/(2\pi)-\left[\tan\theta_s+\tan\theta_v+sqrt(\tan^2\theta_s+\tan^2\theta_v-2\tan\theta_s\tan\theta_v\cos\phi)\right]/\pi \tag{2}$$

$$f_2(\theta_s,\theta_v,\phi)=[1/(\cos\theta_s+\cos\theta_v)][4/(3\pi)][(\pi/2-\xi)\cos\xi+\sin\xi]-1/3 \quad (3)$$

where θ_s, θ_v, ϕ are the solar zenith angle, viewing zenith angle and relative azimuth angle, respectively; $\cos\xi=\cos\theta_s\cos\theta_v+\sin\theta_s\sin\theta_v\cos\phi$; k_0 is the bidirectional reflectance for $\theta_s=\theta_v=0$, k_1 is the weight for geometric scattering kernel function f_1 and k_2 is the weight for volume scattering kernel function f_2. This semi-empirical model can be also applicable to heterogeneous surfaces, and it has been used to generate BRDF dataset for POLDER instrument on ADEOS-I [10].

Since Roujean BRDF is linear and consist of only three parameters, inversion of equations (1) together with (2), (3) is simple in comparison with many complex physical models. Currently, five images are used in bidirectional reflectance modeling. Since total of 31 images spans over nine years, images used in modeling are not continuously taken.

D. Normalization of Bidirectional Reflectance Factor

To normalize BRF at varying angles is to obtain reflectance at standardized sun-target-sensor geometry, such as a specific solar zenith angle and nadir view [4]. In this study, mean solar zenith angle over 31 SPOT images and nadir view is used. Then normalized reflectance (NR) is computed after normalization of BRF.

E. Method evaluation

In order to evaluate the performance of normalization method, a pseudo-invariant area needs to be selected. After carefully visualizing all 31 surface reflectance images by playing movies, an urban area near front exit of Taiwan Railway Station, Tainan is selected. Normalized reflectance in this urban area should be more stable than BRF for all images, no matter what atmospheric and angular effects are.

The performance of normalization method is evaluated by normalization efficiency (NE), which is defined as coefficient of variation (CV) relatively reduced:

$$NE = -(CV_{NR}-CV_{BRF})/ CV_{BRF}*100\% \quad (4)$$

where CV_{NR} and CV_{BRF} are both defined from BRF across different viewing angles for NR and BRF at different bands.

III. Results and Discussion

Urban BRF obtained after AC, shows prominent bidirectional effect across different viewing angles (Fig. 1-Fig. 3). Variation of BRF at varying viewing zenith angle is quite obvious with larger value in backscattering region, i.e. negative viewing zenith angle and lower value in forward-scattering region for building.

Mean urban BRF in selected urban area are 0.123, 0.129 and 0.169 at green, red and NIR bands. They are 0.120, 0.127 and 0.168 for Roujean BRDF normalized reflectance. Standard deviations of BRF at different viewing zenith angles are 0.019, 0.018 and 0.024 at green, red and NIR bands, respectively (Table 1) and those of Roujean BRDF NR are 0.012, 0.012 and 0.013 at green, red and NIR bands, respectively. Hence, they are all reduced when NR are used as BRF is normalized by Roujean BRDF model. Standard deviations are most reduced at NIR band.

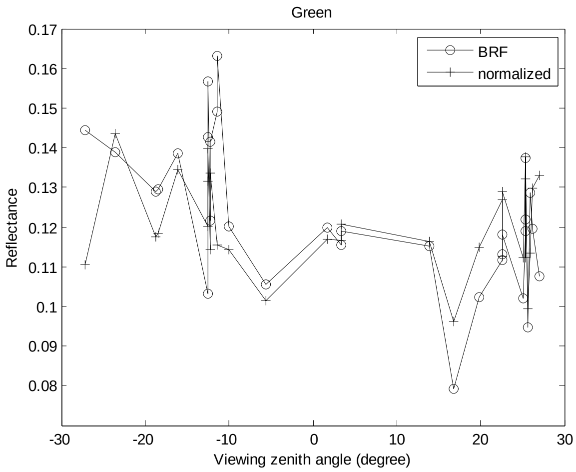

Fig. 1. BRF and NR relative to viewing zenith angles at green band for pseudo-invariant urban area.

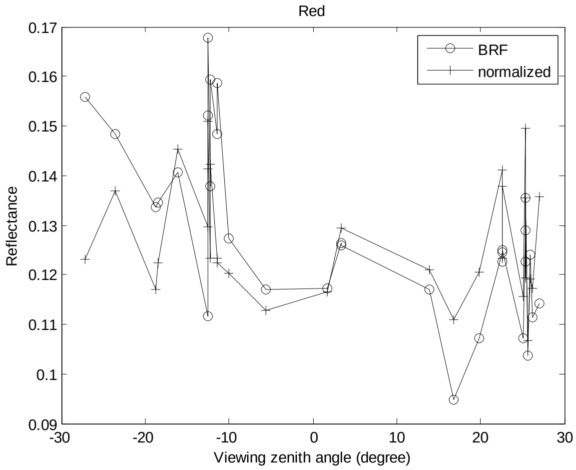

Fig. 2. Similar to Fig. 1, except at red band.

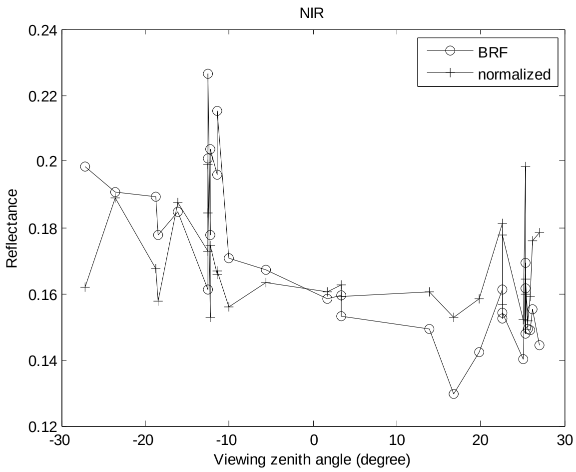

Fig. 3. Similar to Fig. 1, except at near-infrared band.

Furthermore, CV_{NR} are all reduced to 9.77%, 9.18% and 7.97% as compared to CV_{BRF}, i.e. 15.1%, 14.0% and 14.1% at all bands. NEs are 35.4%, 34.4% and 43.7% at green, red and bands, respectively (Table 1), which indicates the success of the normalization procedure.

Table 1 Coefficient of variation (CV) in percentage (%) for BRF and NR as well as NE in percentage (%) defined as reduced CV for different bands.

Band	BRF			Normalized Reflectance			
	Mean	Std	CV_{BRF}	Mean	Std	CV_{NR}	NE
Green	12.29	1.86	15.13	12.03	1.18	9.77	35.4
Red	12.91	1.81	13.99	12.71	1.17	9.18	34.4
NIR	16.9	2.39	14.16	16.8	1.34	7.97	43.7

IV. CONCLUSION

In this study, a normalization method from multi-temporal satellite images is developed and evaluated by using pseudo-invariant area. Roujean BRDF is applied to normalize the BRF after AC. Normalized reflectance is standardized to nadir view and mean solar zenith angle. The results show that normalized urban reflectance can be derived by the method. Coefficients of variation of BRF at different view angles are relatively reduced to over 34% at green, red and bands, which indicates the success of the normalization procedure.

ACKNOWLEDGEMENT

Thanks go to Prof. Neng-Huei Lin in department of atmospheric sciences, National Central University and Prof. Po-Hsiung Lin in department of atmospheric sciences, National Taiwan University, all in Taiwan, R.O.C, for their support of AERONET data.

REFERENCES

[1] C. M. Mertes, A. Schneider, D. Sulla-Menashe, A. Tatem, and B. Tan, "Detecting change in urban areas at continental scales with MODIS data," *Remote Sens. Environ.*, vol. 158, pp. 331–347, 2015.

[2] E. Cubi, N. F. Zibin, S. J. Thompson, and J. Bergerson, "Sustainability of rooftop technologies in cold climates: Comparative life cycle assessment of white roofs, green roofs, and photovoltaic panels," *J. Ind. Ecol.*, vol. 20, no. 2, pp. 249–262, 2016.

[3] C. B. Schaaf *et al.*, "First operational BRDF, albedo nadir reflectance products from MODIS," *Remote Sens. Environ.*, vol. 83, no. 1–2, pp. 135–148, 2002.

[4] C. H. Liu, "A normalization scheme of bidirec-tional reflectances and normalized vegetation indices for short-term multi-angular SPOT satellite images," *J. Mar. Sci. Technol.*, vol. 11, no. 4, pp. 205–212, 2003.

[5] J.-L. Roujean, M. Leroy, and P.-Y. Deschamps, "A bidirectional reflectance model of the Earth's surface for the correction of remote sensing data," *J. Geophys. Res. Atmospheres 1984–2012*, vol. 97, no. D18, pp. 20455–20468, 1992.

[6] B. N. Holben *et al.*, "AERONET—A federated instrument network and data archive for aerosol characterization," *Remote Sens. Environ.*, vol. 66, no. 1, pp. 1–16, 1998.

[7] S. Y. Kotchenova, E. F. Vermote, R. Matarrese, F. J. Klemm Jr, and others, "Validation of a vector version of the 6S radiative transfer code for atmospheric correction of satellite data. Part I: Path radiance," *Appl. Opt.*, vol. 45, no. 26, pp. 6762–6774, 2006.

[8] C.-H. Liu and G.-R. Liu, "Aerosol optical depth retrieval for SPOT HRV images," *J Mar Sci Technol*, vol. 17, no. 4, pp. 300–305, 2009.

[9] Y. J. Kaufman, A. E. Wald, L. A. Remer, B.-C. Gao, R.-R. Li, and L. Flynn, "The MODIS 2.1-/spl mu/m channel-correlation with visible reflectance for use in remote sensing of aerosol," *IEEE Trans. Geosci. Remote Sens.*, vol. 35, no. 5, pp. 1286–1298, 1997.

[10] W. Lucht and P. Lewis, "Theoretical noise sensitivity of BRDF and albedo retrieval from the EOS-MODIS and MISR sensors with respect to angular sampling," *Int. J. Remote Sens.*, vol. 21, no. 1, pp. 81–98, 2000.